Ninth International Conference on Computational Fluid Dynamics (ICCFD9), Istanbul, Turkey, July 11-15, 2016 **ICCFD9-xxxx**

Inclined slot jet impinging on a moving wall

Benmouhoub Dahbia & Mataoui Amina

USTHB, Laboratoire de mécanique des fluides théorique et appliquée, Faculté de physique, Université des sciences et de la technologie Houari Boumediene, B.P 32. Bab Ezzouar 16111 Al Alia, Alger, Algérie.

Corresponding author: benmouhoub_d@yahoo.com & mataoui_amina@yahoo.fr

Abstract: In this work, heat transfer from moving wall due an inclined plane turbulent jet has been numerical investigated. The inclination of nozzle is required for the control of stagnation point location. The numerical predictions are based on RSM second order turbulence model, coupled with enhanced wall treatment. For a given impinging distance of 8 nozzle thickness (8e) and a Reynolds number of 10600,the main parameter of this study is the surface-to-jet velocity ratio Rsj varying from 0 to 1.75, requiring a jet inclination between 0° to 25°.The calculations are in good agreement with available data. The numerical results show that heat transfer is greatly influenced by moving wall effect. The local Nusselt number decreases with increasing surface-to-jet velocity ratios (R_{sj}=1). However, the accurate inclination of the jet enhances heat transfer and recovers the stagnation point location, of the interaction on a stationary wall.

Keywords: Inclined slot jet, Moving wall, CFD, Heat transfer, Nusselt number, stagnation point location.

1 Introduction

Heat transfer by impinging jet are encountered in many industrial applications such as tempering and shaping glass, draying textiles and paper, cooling of electronic components and turbine blades, and annealing of continuous sheets of materials, etc. Particular interests were devoted to impinging jets due to their characteristics of heat and mass transfer. Impinging jet on a moving wall were little bit investigated compared to the case of immobile wall. Among work implying a plane turbulent air jet impinging a moving wall, we quote the experimental studies of Subba Raju and Schlünder [1] of Van Heiningen [2] and Senter [3] or the numerical studies of Chattopadhay et al [4, 5], Huang et al [6], Sharif et al [8], Aghahani et al [9] and Benmouhoub and Mataoui [10]. All these works have reported the effect of the impingement surface motion on the flow field and heat transfer. The movement of the impacted wall causes the displacement of stagnation point and reduces its heat transfer.
Senter [3], from measurements of the case of perpendicular jet impingement on a mobile wall, has examined the inclined case of in order to recover the characteristics of perpendicular impingement.

Indeed, for Reynolds number of 10600 and surface-to-jet velocity ratio of 1, Senter [3] confirmed an improvement of the Nusselt average number of 25% for a jet inclination of 8°.
In this paper, we present the results of preliminary study in order to find the accurate inclination giving the stagnation point location of orthogonal jet impinging an immobile wall

2 Problem Statement

2. 1 Geometry of problem

The geometry and boundary condition are summarized in figure (1). The flow is steady in average and fully turbulent. The fluid (air) is incompressible with constant thermo-physical properties. The jet exit velocity is V_j. The moving wall is moving with velocity U_0 corresponding to the surface-to-jet velocity ratio R_{sj} defined by: $R_{sj} = U_0 / V_j$. The jet at the exit is maintained at ambient temperature T_C, while the moving wall is heated at T_H (T_C=293K and T_H=313K).
Furthermore due to the jet inclination, the velocity components are:
$U = V_j.\cos(\alpha)$; $V = V_j.\sin(\alpha)$ and
Kinetic energy and dissipation rate are deduced from jet parameters as follows:

$k = I.V_j^2$ where $I = 0.02$ and $\varepsilon = \dfrac{k^{3/2}}{0.03e}$

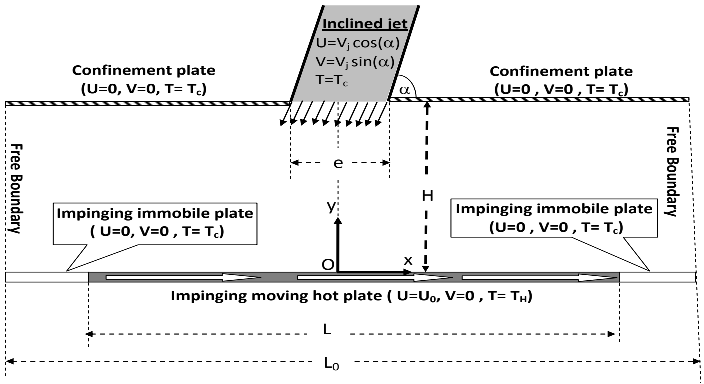

Figure1: Configuration and boundary conditions.

2. 2 Governing equations

Mass, momentum, and energy conservation equations for incompressible flow, constant fluid properties and steady state conditions are as follows:
Mass conservative equation:

$$\frac{\partial U_i}{\partial x_i} = 0 \qquad (1)$$

Momentum conservation equation:

$$U_j \frac{\partial U_i}{\partial x_j} = \frac{\partial}{\partial x_i}\left(\frac{P}{\rho}\right) + \frac{\partial}{\partial x_j}\left(\nu \frac{\partial U_i}{\partial x_j} - \overline{u_i u_j}\right) \qquad (2)$$

Energy conservation equation:

$$U_i \frac{\partial T}{\partial x_i} = \frac{\partial}{\partial x_i}\left(\gamma \frac{\partial T}{\partial x_i} - \overline{u_i \theta}\right) \qquad (3)$$

2. 3 Turbulence modeling

In equations (2) and (3), Reynolds stress component $\overline{u_i u_j}$ and turbulent heat flux $\rho\overline{u_i\theta}$ require modeling. The closure of these equations is achieved by means of linear strain pressure - Reynolds stress second order model. This model does not require eddy viscosity hypothesis. The differential equation Reynolds stress transport consists of standard Reynolds stress model based on dissipation equation ε. There are three versions of the standard Reynolds stress models. They are called: LRR-IP, LRRQI and SSG. Reece and Rodi [11] developed the LRR-IP and LRR-QI models. The pressure-strain expression consists of an anisotropy tensor, mean strain rate tensor and vorticity tensor. The production due to the buoyancy is neglected in this study.
By analogy with molecular transport, for all models (first or second order models), the Simple Gradient Diffusion Hypothesis (SGDH) is used. The following algebraic constitutive law is allows deducing the velocity-temperature correlation:

$$\overline{u_i\theta} = \gamma_t \frac{\partial T}{\partial x_j}$$

$$\text{where} \quad \gamma_t = \frac{\nu_t}{\Pr_t} \quad \text{and} \quad \nu_t = C_\mu \frac{k^2}{\varepsilon} \tag{4}$$

Near the wall, specific treatment is required. After several tests, enhanced wall treatment predicts the flow fields with a best accuracy [12].

2. 4 Numerical procedure

The numerical predictions based on finite volume method are performed by ANSYS FLYENT 14.0 CFD code. The discritisation of each equation is achieved on collocated meshes. The algorithm SIMPLEC is applied for pressure-velocity coupling. For the interpolation of convection-diffusion terms: second order scheme for pressure and POWER LAW scheme for the other variable, are applied Patankar [13].

2. 4. 1 Grid arrangement

A two dimensional structural non-uniform grid is generated. The enhanced wall treatment is used, requiring a fine grid size in the vicinity to each wall (Fig. 2)

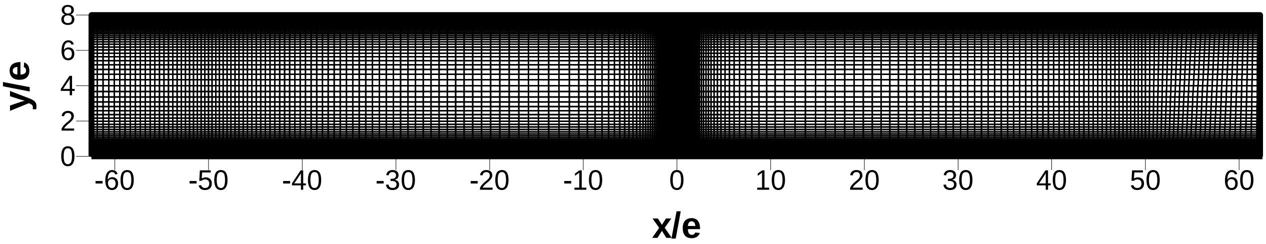

Figure 2: Typical grid arrangement

Several grids were tested in order to examine their independence on the solution. Fig. 3 shows the effect of cells size on the evolution of local Nusselt number. It is noticed that the independence of the grid on the solution is obtained for 290 x 90 nodes beyond which no further signification change is observed. This grid distribution is therefore used in all calculations knowing that all geometrical parameters are not modified.

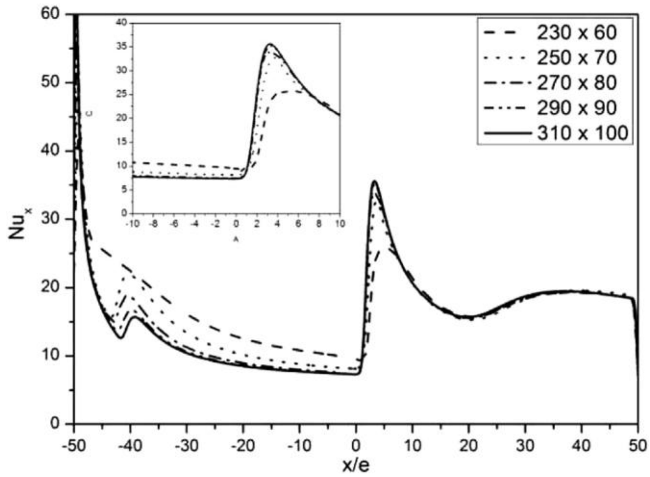

Figure 3: Effect of grid refinement on local Nusselt number along the moving wall. Re=10000, R_{sj}=1 H/e=8, α=0.

2. 4. 2 Validation

The validation of numerical technique is checked on the dynamic and thermal fields. The normalized velocities (U/V_j) and (V/V_j) for two cross sections (y=0.3 and 4) for two velocity ratios: Rsj=0, α=0 and Rsj=1, α=9° and Re=10600, were compared to PIV experimental data of Senter [3]. As shows figure 4, a good agreement was obtained. Figure 5 also shows a good agreement with the experimental data of Gardon and Akfirat [14] for the case of an immobile wall corresponding to R_{sj}=0, α=0°, H/e=8 and Re=11000.

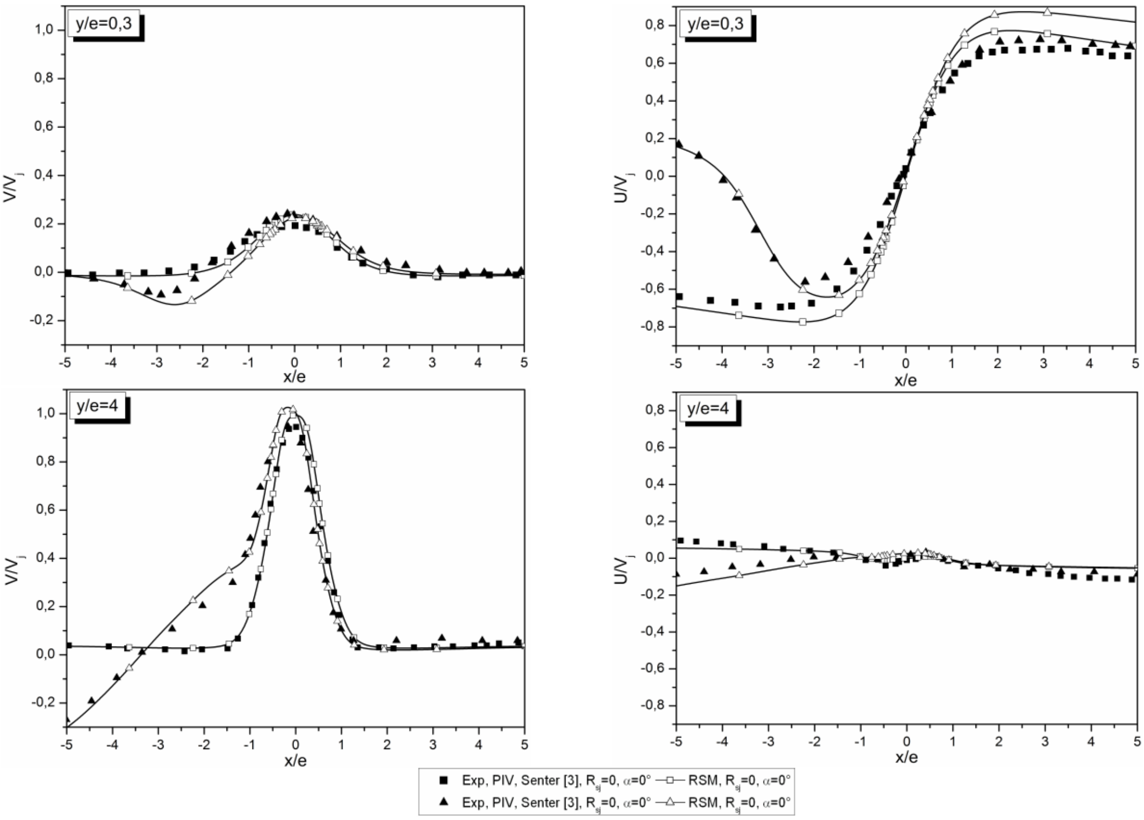

Figure 4: Validation; mean velocity components U/V_j and V/V_j , Re=10600, for horizontal section y/e=0.3 and 4.

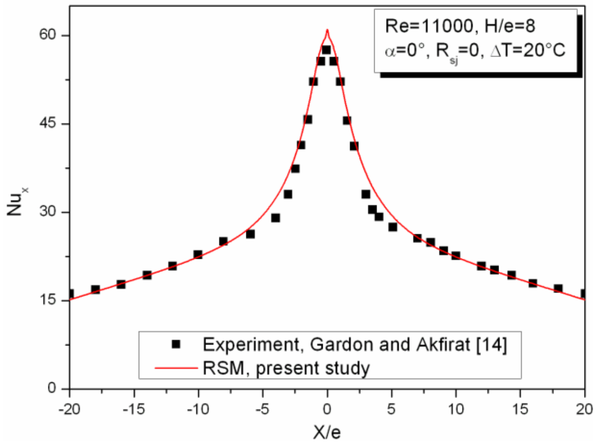

Figure 5: Comparison of local Nusselt number prediction with the experiment data of Gardon and Akfirat [14]

3 Results and Discussion

Figure (6) shows the streamlines contours for Re=10600, for the cases of surface-to-jet velocities ratios such $0 \leq R_{sj} \leq 1.75$ and their corresponding inclined cases which allow to get the case of a jet impinging perpendicularly on a stationary wall ($0° \leq \alpha \leq 25°$). All results are compared to those of available experimental measurements (PIV) [3]. A good agreement is obtained with PIV measurement [3] excepting the cases where $0 \leq R_{sj} \leq 1$.

For $R_{sj}=0$, $\alpha=0°$, relating to stationary plate, the flow topology is perfectly symmetric relative to the jet axis. Two identical eddies are observed, they are generated by the flow driving and by the upper wall confinement.

When the wall moves from left to right $0 < R_{sj} \leq 1$, a third contra-rotating eddy appears at the left part of the moving wall. This new recirculation reduces the size of the left principal vortex and thus the jet is deviated towards the right part of the mobile wall. The location of the stagnation point is therefore shifted. For $R_{sj} > 1$, the jet is completely deviated by the movement of the wall. The jet does not attain the moving wall and its streamlines become progressively parallel to the wall when the surface-to-jet velocities ratio increases. The shear drives the flow by the moving wall is much larger than that of the left region.

The inclination of the nozzle is required in order to recover the case of jet impinging perpendicularly to stationary wall. These inclinations are obtained following several tests. When the velocity ratio increases, the suitable inclination of the jet augments.

Figure (7) illustrates a comparison for each components of the average velocity U/Vj and U/ Vj, between the inclined and orthogonal cases, through the cross section y/e = 0.3. From this figure, for $0 < R_{sj} \leq 1$: we observe a good similarity of the value of orthogonal jet impinging on a fixed surface and those of the inclined jet interaction on a moving surface in the stagnation points region. However, for $1 < R_{sj} \leq 1.75$, the profiles are different. For this range of velocity ratio, the flow is parallel to the wall even with the inclination of the nozzle; the jet does not hit the moving wall.

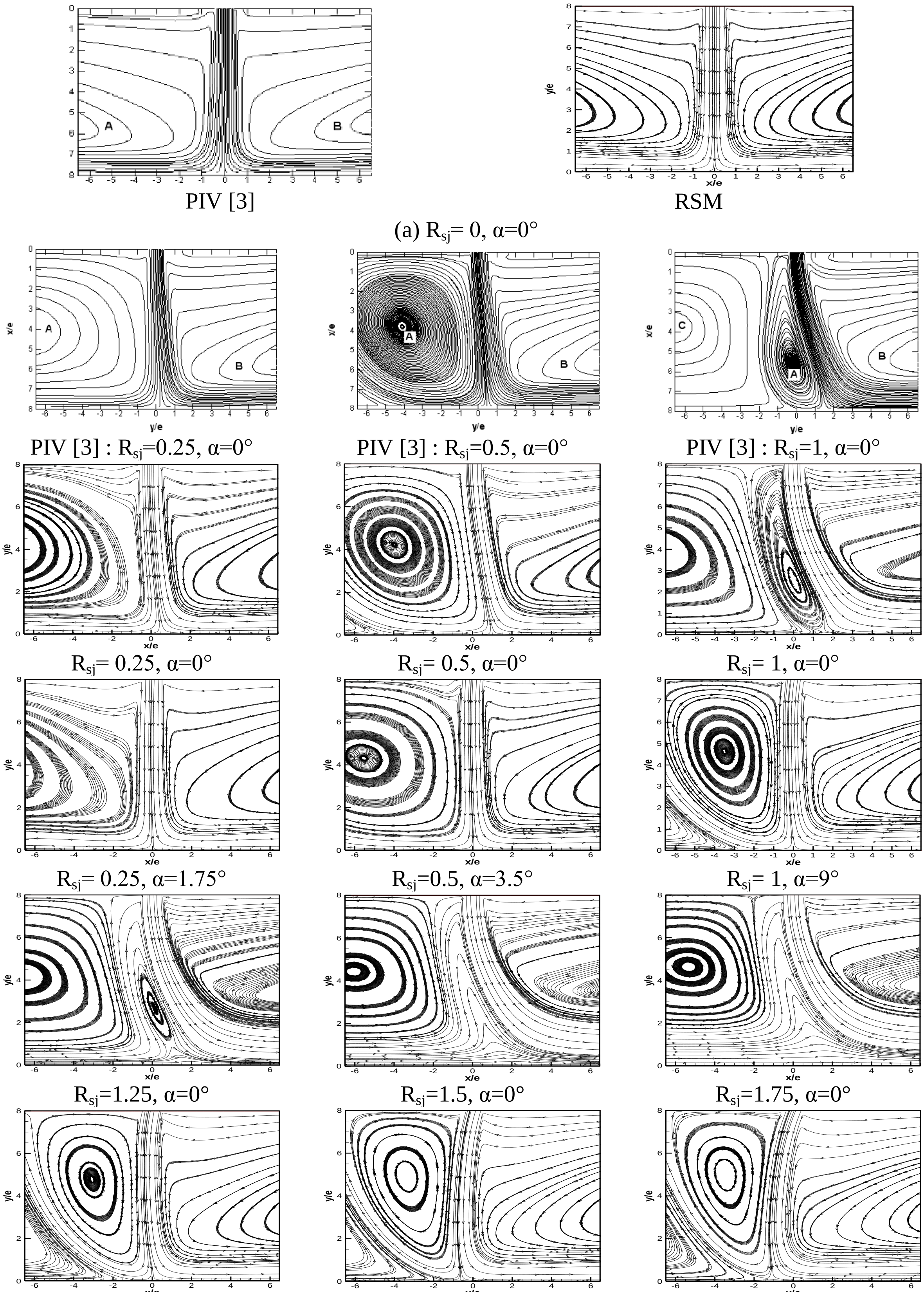

PIV [3]

RSM

(a) R_{sj}= 0, α=0°

PIV [3] : R_{sj}=0.25, α=0°

PIV [3] : R_{sj}=0.5, α=0°

PIV [3] : R_{sj}=1, α=0°

R_{sj}= 0.25, α=0°

R_{sj}= 0.5, α=0°

R_{sj}= 1, α=0°

R_{sj}= 0.25, α=1.75°

R_{sj}=0.5, α=3.5°

R_{sj}= 1, α=9°

R_{sj}=1.25, α=0°

R_{sj}=1.5, α=0°

R_{sj}=1.75, α=0°

R_{sj}=1.25, α=12°

R_{sj}=1.5, α=17.75°

R_{sj}=1.75, α=25°

(b) $R_{sj} \neq 0$, $\alpha \neq 0°$

Figure 6: Streamlines contours: effect of plate velocity ratio and inclination angle Re=10600; $0 \leq Rsj \leq 1.75$; $0° \leq \alpha \leq 25°$

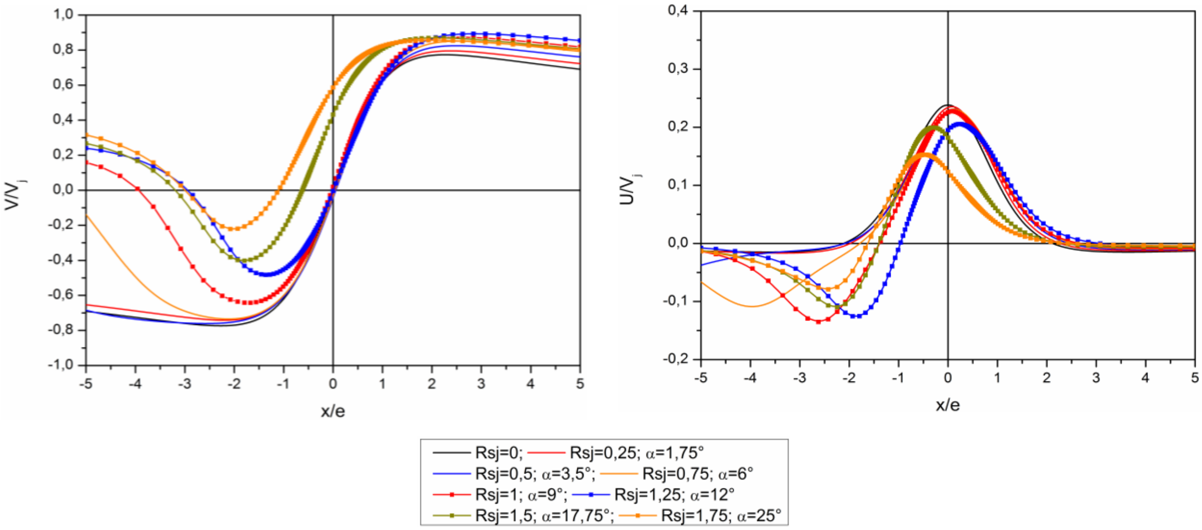

Figure 7: Effect of the inclination of the jet on transverse profiles of average velocity U/V_j and $U/\ V_j$ Re=10600, y/e=0.3.

The dimensionless Nusselt number defines the heat transfer of fluid along the heated impinging wall, which characterizes the ratio of convective to conductive heat transfer across the corresponding wall. The local Nusselt number distribution over the impingement wall is defined in Eq.5:

$$Nu(x) = -\left(\frac{e}{T_H - T_C}\right)\left(\frac{\partial T}{\partial n}\right)_{ywall} \quad (5)$$

Where *n* is the perpendicular direction to the corresponding wall.

Figure 8(a) shows the evolution of local Nusselt number Nu(x) along the moving plate for Re=10600 and for various values of R_{sj}. It is observed from this figure that, for stationary plate (R_{sj}=0), the curve is symmetrical, it is characterized by a maximum at the stagnation points which are located on the jet axis. On either side of this axis the local Nusselt number decreases gradually. While for the case of moving wall $R_{sj} \neq 0$, we note a peak appears at the left end of the impinging wall (x/e=-50), which augments when R_{sj} increases. The development of this maximum can be explained by the velocity discontinuity between the moving part and the left immobile wall part [3].

For the cases: $0.25 \leq R_{sj} \leq 1$

The maximum value decreases and its position is deflected in the same direction as the moving wall, this is due to the shear generated by plate movement. A drop occurs in the left part of the plate. This reduction is related with the apparition of the new recirculation [3]. Local Nusselt number augments on the right part of the plate when R_{sj} increases by the effect of the progressive jet deviation (Benmouhoub and Mataoui[9]).

For $R_{sj} > 1$

For these cases, the plate velocity exceeds that of the jet. The maximum value of local Nusselt number progressively disappears at the left side of the wall. The Nu(x) increases significantly, this is due to the shear generated by the movement of the wall.

Figure 8 (b) illustrates the distribution of the local Nusselt number for each surface-to-jet velocity ratio R_{sj}, the inclined jet is in the opposite direction to the movement of the wall with an suitable angle to reach the maximum at the same point as the orthogonal impact jet on an immobile wall. It was found that the inclination of the nozzle increases with increasing velocity ratio R_{sj}. The value of the local Nusselt number at the stagnation point increases compared to the case of the vertical jet (Fig. 9).

Table 1 shows the increasing percentage of local Nusselt at the stagnation points between the two cases (inclined and non-inclined jet).

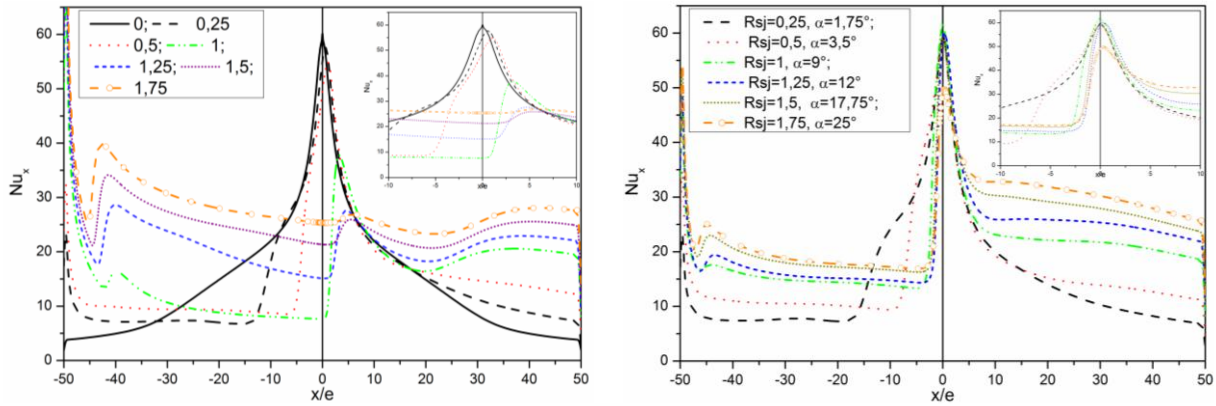

(a) (b)

Figure 8: Distribution of local Nusselt number along the hot moving wall for Re=10600: (a) perpendicular jet; (b) inclined jet [9]

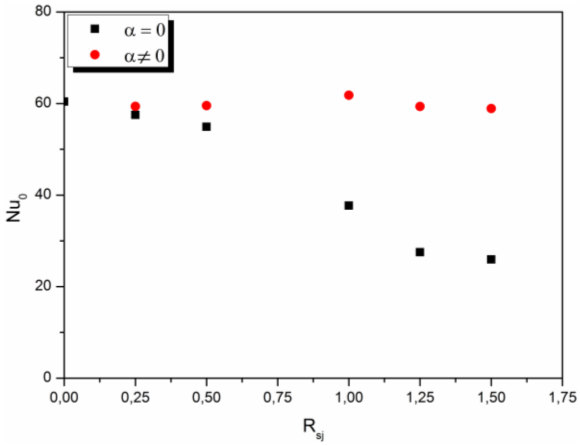

Figure 9: Nusselt number at stagnation point Re=10600.

Table 1. Gain of local Nusselt number at stagnation points

R_{sj}	0.25	0.5	0.75	1	1.25	1.5	1.75
δ(%)	3.884	8.554	19.735	63.834	116.772	126.759	84.729

4 Conclusion

The global structure and heat transfer due to confined slot jet impinging on a moving wall was investigated numerically for a given range of plate velocity ratios and jet inclination. The RSM turbulence model with enhanced wall treatment for near wall turbulence modeling is used. Results are in good agreement with previous experimental measurement. For Rsj ≠ 0, the deviation of the stagnation point from the jet exit axis generates an important variation of the heat transfer. With increasing velocity plate ratio, the magnitude of maximum local Nusselt number decreases and its position is deviated in the direction of movement of the wall. However, the accurate inclination of the jet in the opposite direction to the movement of the wall considerably improves local heat transfer in the region of the stagnation point.

References

[1] Subba Raju, K., & Schlünder, E. U. (1977). Heat transfer between an impinging jet and a continuously moving surface. *Wärme-stoffübertr*, *10*, 131-136.

[2] Van Heiningen, A. R. P., Mujumdar, A. S., & Douglas, W. J. M. (1977). Flow and heat transfer characteristics of a turbulent slot jet impinging on a moving wall. In *Symposium on Turbulent Shear Flows* (Vol. 1, pp. 3-9).

[3] Senter, J,. Senter. Analyse experimentale et numérique des écoulements et des transferts de chaleur convectifs produits par un jet plan impactant une plaque plane mobile. Phd, thesis Université de Nanates, France, 2006.

[4] Chattopadhyay, H., Biswas, G., & Mitra, N. K. (2002). Heat transfer from a moving surface due to impinging slot jets. *Journal of heat transfer*, *124*(3), 433-440.

[5] Chattopadhyay, H., & Saha, S. K. (2003). Turbulent flow and heat transfer from a slot jet impinging on a moving plate. *International Journal of Heat and Fluid Flow*, *24*(5), 685-697.

[6] Huang, P. G., Mujumdar, A. S., & Douglas, W. J. M. (1984). Numerical prediction of fluid flow and heat transfer under a turbulent impinging slot jet with surface motion and crossflow. *ASME paper*, (84-WA), 1-8.

[7] Sharif, M. A. R., & Banerjee, A. (2009). Numerical analysis of heat transfer due to confined slot-jet impingement on a moving plate. *Applied Thermal Engineering*, *29*(2), 532-540.

[8] Aghahani, M., Eslami, G., & Hadidi, A. (2014). Heat transfer in a turbulent jet impinging on a moving plate considering high plate-to-jet velocity ratios. *Journal of Mechanical Science and Technology*, *28*(11), 4509-4516.

[9] Benmouhoub, D., & Mataoui, A. (2015). Inclination of an impinging jet on a moving wall to control the stagnation point location. *International Journal of Thermal Sciences*, *89*, 294-304.

[10] Mobtil, M., Bougeard, D., & Solliec, C. (2014). Inverse determination of convective heat transfer between an impinging jet and a continuously moving flat surface. *International Journal of Heat and Fluid Flow*, *50*, 83-94.

[11] Launder, B. E., Reece, G. J., & Rodi, W. (1975). Progress in the development of a Reynolds-stress turbulence closure. *Journal of fluid mechanics*, *68*(03), 537-566.

[12] Kader, B. A. (1981). Temperature and concentration profiles in fully turbulent boundary layers. *International Journal of Heat and Mass Transfer*, *24*(9), 1541-1544.

[13] Patankar, S. V. (1980). Numerical heat transfer and fluid flow: Computational methods in mechanics and thermal science.

[14] Gardon, R., & Akfirat, J. C. (1966). Heat transfer characteristics of impinging two-dimensional air jets. *Journal of Heat Transfer*, *88*(1), 101-10.